Chapter 8
Electrically Conductive Polymer Nanocomposites

Thomas Gkourmpis

8.1 Introduction

Polymer nanocomposites combine the properties of the matrix with those of the filler additive, thus allowing for the creation of totally new classes of materials with improved mechanical, electrical, optical and thermal properties. This combination of properties offers immense versatility and design capabilities and as consequence research in nanocomposites has been ever-growing. Traditionally carbon black has been the filler of choice for applications where electrical conductivity was required. This was done mainly due to the simplicity and versatility of the carbon black particles in combination with the relatively low cost preparation methods available (Kuhner and Voll 1993). Over the years other conductive fillers of anisotropic dimensions (high aspect ratio) like metal nanowires, graphene and carbon nanotubes (CNTs) have been introduced leading to a revolution in polymer nanocomposites. The potential of these fillers to achieve high conductivity due to their unique geometry at low or very low concentrations has attracted enormous scientific and commercial attention.

In order for this potential to be realised the possibility of producing and controlling well-defined systems is dependent on the detailed understanding of the structure–property relations of these nanocomposites. In this section we will review systems where the filler introduced creates a level of electrical conductivity in the resulting composition, and we will discuss how different classes of fillers affect the overall properties of the polymer. Furthermore, we will discuss the key structure–property relationships highlighting the underlying mechanisms that give rise to them. Of course such a wide topic cannot be treated within the limitations of this work, so the interested reader is encouraged to explore a number of comprehensive

T. Gkourmpis
Innovation and Technology, Borealis AB, Stenungsund SE 444-86, Sweden
e-mail: thomas.gkourmpis@borealisgroup.com

G.R. Mitchell, A. Tojeira (eds.), *Controlling the Morphology of Polymers*,
DOI 10.1007/978-3-319-39322-3_8

studies on polymer nanocomposites available (Bauhofer and Kovacs 2009; Moniruzzaman and Winey 2006; Winey and Vaia 2007; Winey et al. 2007; Byrne and Gunko 2010; Mutiso and Winey 2012; Gkourmpis 2014).

8.2 Percolation Theory

The connectivity and spatial arrangement of objects within a network structure and the resulting macroscopic effects can be described by the percolation theory. In all its variations the percolation theory focuses on critical phenomena that originate from the spatial formation of a network and result in sharp transitions in the behaviour of the system of interest (Kirkpatrick 1973). Percolation models have been applied with various degrees of success to the description of the electrical behaviour of polymer nanocomposites. In these systems the insulating polymer matrix is loaded with conductive filler whose network formation leads to a sharp insulation-conductor transition (Lux 1993). Experimental work and theoretical predictions have established that the system's conductivity σ follows a power-law dependence in accordance with percolation theory

$$\sigma \approx \sigma_{\mathrm{o}}(\phi - \phi_{\mathrm{C}})^{t}$$

with σ_{o} a pre-exponential factor that is dependent on the conductivity of the filler, the network topology and the types of contact resistance. The terms ϕ and ϕ_{C} correspond to the filler concentration and the critical concentration at the transition (also known as percolation threshold) (Foygel et al. 2005). The critical exponent t is also conductivity-dependant with universal values of $t \approx 1.33$ and $t \approx 2$ for two and three dimensions, respectively (Stauffer and Aharony 1987; Sahimi 1994). It must be noted however that a wide range of values as high as $t \approx 10$ for the critical exponent have been reported (Bauhofer and Kovacs 2009; Gkourmpis 2014). The reason for this deviation from universality is still not well understood with complex tunnelling transport phenomena (Balberg 1987, 2009; Grimaldi and Balberg 2006; Johner et al. 2008) and filler variability in terms of production, entanglement, interconnections and surface chemistry being suggested as possible culprits (Mutiso and Winey 2012). In Fig. 8.1, the percolative behaviour of a system of polycarbonate with single-walled carbon nanotubes can be seen (Ramasubramaniam et al. 2003). This behaviour of sharp conductivity increase at a specific filler concentration is typical of all polymer nanocomposites and can be understood within the framework of the percolation theory.

As discussed previously, there are a number of percolation models dealing with electrical conductivity. Initial approaches were treated with systems where the particles were confined in well-defined periodic positions (lattice models). For such systems analytical solutions can be used in the case of one and two dimensions (Fisher and Essam 1961) and numerical solutions based on Monte Carlo methods for three dimensions (Kirkpatrick 1973). Obviously such models despite their

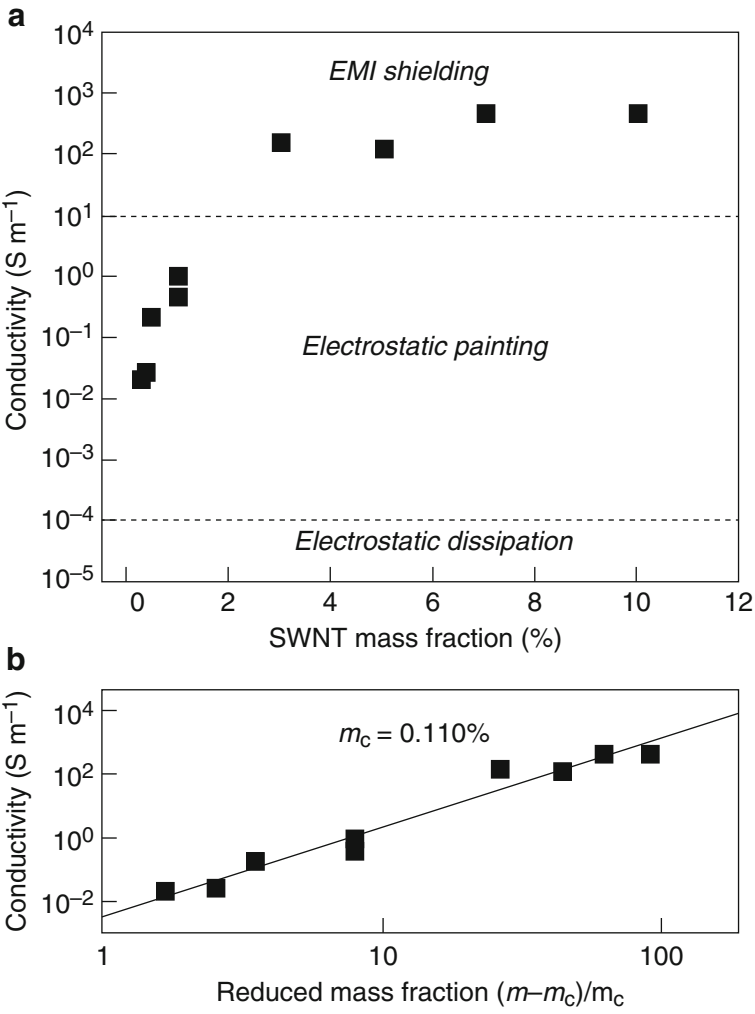

Fig. 8.1 (**a**) Electrical conductivity of polycarbonate/SWCNT composites as a function of the filler mass fraction. Different commercial applications are also noted in the graph. (**b**) Power-law application to experimental data for the calculation of the percolation threshold. Reprinted with permission from Ramasubramaniam et al. (2003)

usefulness are very poor representations of real systems, something that has led to the development of continuum (off-lattice) models that allow more realistic placement of the particles in space. The main types of continuum models can be classified as follows:

Soft-core systems: In this class of models the particles are assumed to be fully interpenetrating and are considered bonded when they overlap.

Hard-core systems: In this approach the particles are allowed to touch each other but not overlap.

Hard-core with soft shell: In this approach the electrical percolation depends not only on the geometry of the particles but on the tunnelling distance between them. In other words the particles are considered to have a hard non-penetrating core and a penetrable shell around the hard core.

For high aspect ratio systems the study gets computationally expensive due to the spatial orientation of the particles. One of the most common approaches to avoid complexity is to treat the particles with respect to their excluded volume (Hard-core) that can be significantly different from their true volume (Balberg et al. 1984). In such a representation the critical number of particles required for percolation N_C is inversely proportional to the excluded volume (V_{excl})

$$N_C \propto \frac{1}{V_{excl}}$$

In a similar manner, the percolation threshold ϕ_C can be expressed as the ratio of the true volume of the particle (V) over the excluded volume

$$\phi_C \propto \frac{V}{V_{excl}}$$

In the case of a cylinder the average excluded volume per rod can be written as (Balberg et al. 1984)

$$V_{excl} = \frac{32\pi}{3}R^3\left[1 + \frac{3}{4}\left(\frac{L}{R}\right) + \frac{3}{8\pi}\langle \sin\theta\rangle\left(\frac{L}{R}\right)^2\right]$$

with L and R the length and radius of the cylinder and θ the angle between two random rods. In a similar manner, the percolation threshold can be expressed as (White et al. 2009)

$$\phi_C = \frac{\frac{4}{3}\pi R^3 + \pi R^2 L}{\frac{32}{2}\pi R^3 + 8\pi R^2 L + \pi R L^2}$$

From these relations we can clearly see that the aspect ratio (L/R) will dominate the percolation threshold, and although in the limit $L/R \to \infty$ the above-mentioned equations require some alterations (Balberg et al. 1984; Berhan and Sastry 2007), the basic assumptions are still valid (Mutiso and Winey 2012). In the case of the hard-core with soft shell cylinders the equivalent relationship can be expressed as (Berhan and Sastry 2007; Wang and Ogale 1993)

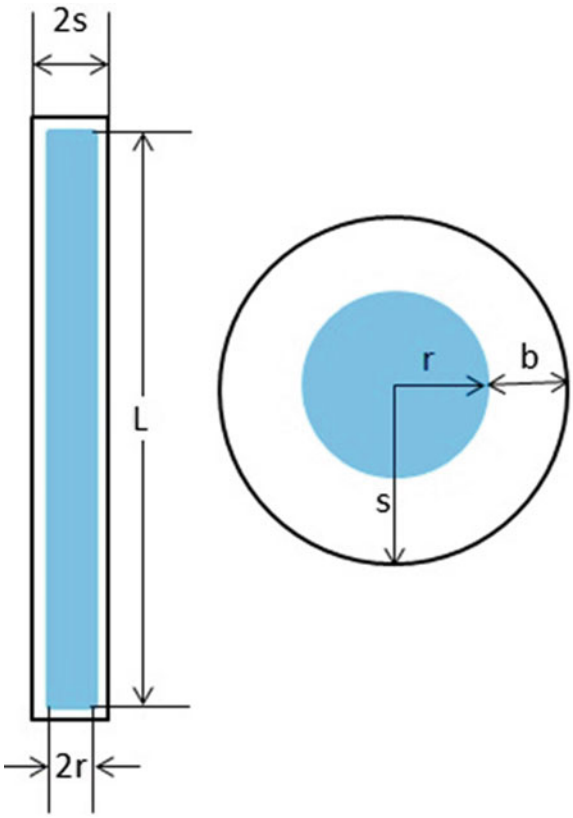

Fig. 8.2 Schematic representation of a rod (*left*) and a sphere (*right*) indicating the impenetrable hard core and the penetrable soft shell

$$V_{\text{excl}} = \frac{32\pi}{3}R^3\left[\left(1-\kappa^3\right)+\frac{3}{4}\left(\frac{L}{R}\right)\left(1-\kappa^2\right)+\frac{3}{32}\left(\frac{L}{R}\right)^2(1-\kappa)\right]$$

with $\kappa = r/s$ being the core–shell ratio (see Fig. 8.2).

Most percolation studies rely on Monte Carlo simulations, whose properties of interest are critical cluster size, bond densities (i.e. number of bonds that lead to network per site), particle volume in the matrix, particle orientation and network geometry at the threshold. In most cases simulations treat the percolation in a statistical manner which means that the particles are randomly distributed in the matrix and network pathways are formed simply by increasing the particle volume fraction in the composite. Although such an approach has merit and provides valuable insight on the network formation, it is far away from reality, especially when polymers are concerned. Addition of particles in a polymer matrix is mainly performed via solution or melt mixing, which means that both particles and polymer chains are in motion and interact with each other. More advanced theoretical approaches do take into consideration the thermodynamic interactions between the composite constituents (particle–particle, particle–polymer and

polymer–polymer) as well as any external stimulus such as shear forces. The need to account for the particle mobility and interactions manifests itself in cases where strongly interacting particles with a tendency to cluster after mixing is considered. A typical example of such system is epoxy/CNT composites whose very low reported and experimentally observed percolation ($\phi_C \ll 0.1\,\mathrm{wt}\%$) is attributed to the strong attractive interactions between the carbon nanotubes (Bauhofer and Kovacs 2009; Mutiso and Winey 2012; Gkourmpis 2014; Bryning et al. 2005).

8.2.1 Electrical Conductivity Mechanisms

Macroscopic conductivity is achieved by addition of conductive particles in an insulating polymer matrix and is controlled by percolative behaviour. The conductivity-filler dependence is typically governed by an s-shape curve with three distinct regimes: (1) at very low loadings the filler amount in the matrix is low and the individual particle density is not enough to create an adequate network for current flow. In this regime the macroscopic (observed) conductivity is dominated by the matrix, (2) close to the percolation threshold the filler concentration is such that an adequate network capable of facilitating current flow is created, and this is followed by a sharp increase in the observed conductivity value and, (3) above the threshold the particle network becomes extensive, thus capable to facilitate current flow through multiple channels, and this is manifested by a high observed conductivity value. Within the framework of the percolation theory the electrical conductivity of a polymer nanocomposite is treated in geometrical terms in each of the three distinct regimes. In other words in order to have current flow through the matrix, the particles must be in contact in such numbers as to have a clear intact pathway (network) whose number or density determines the overall value of the conductivity. In the case where the particles are far apart with enough polymers occupying the space between them, no current flow is possible and the system is not conductive. A schematic representation of these ideas can be seen in Fig. 8.3.

Here we must note that even in the insulating region there is a certain level of conductivity despite the lack of adequate conductive network. The conductivity in this region is dominated by trapped charge carriers and polarisation effects and is mainly influenced by the morphology, polarity and electronic band structure of the polymer. Furthermore due to the frequency dependence of conductivity and permittivity of the matrix, the dielectric response of the system will be different for direct and alternating current. Nevertheless, this type of conductivity of essentially insulating materials is beyond the scope of this work but the interested reader is encouraged to consult recently published reviews and the references wherein (Glowacki et al. 2012).

It has been reported that filler particles can be separated by polymer at the high conductive region as well as in the insulating region (Balberg 2009). For electrical conductivity to exist in this case it has been suggested that the electric transport between the conductive particles is facilitated by quantum tunnelling and electronic

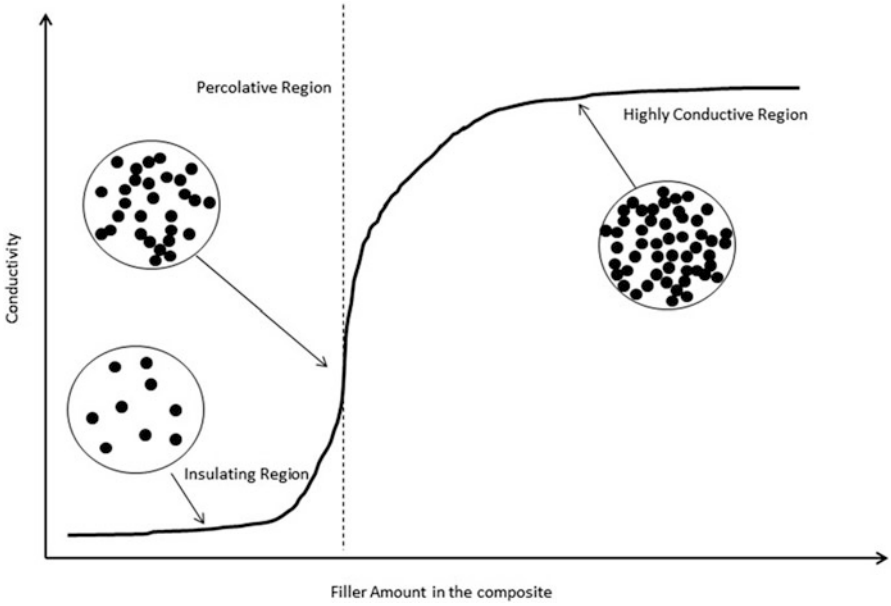

Fig. 8.3 Schematic representation of the percolative behaviour of a nanocomposite, indicating the different regions as a function of the electrical conductivity and the total amount of filler present. A schematic representation of the network creation for artificial spherical particles can also be seen for the different conductivity regions

hoping mechanisms (Balberg 1987, 2009, 2012; Glowacki et al. 2012; Strumpler and Glatz-Reichenbach 1999; Balberg et al. 2004; Sherman et al. 1983). Here we must note that while the percolation theory requires a sharp cut-off as onset to conductivity (i.e. the particles will either touch and conduct or be apart and not conduct) the tunnelling approximation is a continuous function of the interparticle distances (Stauffer and Aharony 1987; Sahimi 1994). Consequently, the tunnelling conductance decays exponentially with the interparticle distance, thus leading to a non-sharp cut-off (Balberg 2009). According to this we can express the interparticle conductance g between two particles i and j as (Balberg 2012; Ambrosetti et al. 2010)

$$g_{ij} = g_{\mathrm{o}} \exp\left(-\frac{2\delta_{ij}}{\xi}\right)$$

with ξ the wavefunction decay length of the electron outside the particle to which it belongs and δ_{ij} the minimal distance between two particles. In the case of spheres of diameter D the minimal distance can be written as $\delta_{ij} = r_{ij} - D$ with r_{ij} the distance between the two centres. In this case we have two extremes that will lead to qualitatively different conductivity behaviours. In the case of large particles $\xi/D \rightarrow 0$ it becomes obvious from the above relationship that non-zero conductance is

possible only when the particles touch each other. Therefore removing particles from the random closed packed limit will be equivalent of removing tunnelling bonds in a similar manner to a standard percolation lattice system (Sahimi 1994; Balberg 2012). In such a case the system will exhibit conductivity that follows percolation-type behaviour with critical exponent $t \approx 2$ and φ_C that correspond to the appropriate system-dependant percolation threshold (Johner et al. 2008). In the other extreme case $D/\xi \to 0$ the sites are randomly distributed in the system and site density ρ variations have no effect on the particle connectivity, but affect the distance $\delta_{ij} = r_{ij}$ between sites (Balberg 2009). In such case it has been seen that the conductivity behaviour in the context of hoping approximation in amorphous semiconductors can be expressed as (Balberg 2012; Ambrosetti et al. 2010)

$$\sigma \propto \exp\left[-\frac{1.75}{(\xi\rho)^{1/3}}\right]$$

which is the low density limit of the first extreme case.

The conductivity behaviour as a function of the percolation threshold and the aspect ratio for spheres, oblate (sheet-like) and prolate (rod-like) spheroids has been calculated using random sequential addition (RSA) and Monte Carlo techniques (Mutiso and Winey 2012; Balberg 2012; Shklovskii and Efros 1984; Tye and Halperin 1989; Berman et al. 1986; Shante and Kirckpatrick 1971; Balberg and Binenbaum 1987; Hunt and Ewing 2009; Ambrosetti et al. 2010). In Fig. 8.4 the distributions of impenetrable spheres and spheroids of different aspect ratio a/b (with a and b the polar and equatorial semi-axes, respectively) can be seen. In this framework the conductivity has been seen to reduce strongly with decreasing volume fraction of the particles (see Fig. 8.5), something attributed to the increasing interparticle distances that lead to a reduction of the local tunnelling conductances (Ambrosetti et al. 2010). This reduction depends strongly on the shape of the filler particles, and with increased anisotropy the overall conductivity onset decreases for a fixed ξ (Fig. 8.5b). Analytical relations for the tunnelling conductivity of randomly distributed prolate, oblate and spherical particles, respectively, can be expressed as (Ambrosetti et al. 2010)

$$\sigma \approx \sigma_o \exp\left[-\frac{2D}{\xi}\frac{\gamma(b/a)^2}{\phi}\right]$$

$$\sigma \approx \sigma_o \exp\left\{-\frac{2D}{\xi}\left[\frac{0.15(a/b)}{\phi}\right]^{4/3}\right\}$$

$$\sigma \approx \sigma_o \exp\left[-\frac{2D}{\xi}\frac{1.65(1-\phi)^3}{12\phi(2-\phi)}\right]$$

In the previous discussion we have seen that the hoping and tunnelling conductivity models are extreme cases of the same problem. Therefore for a system with

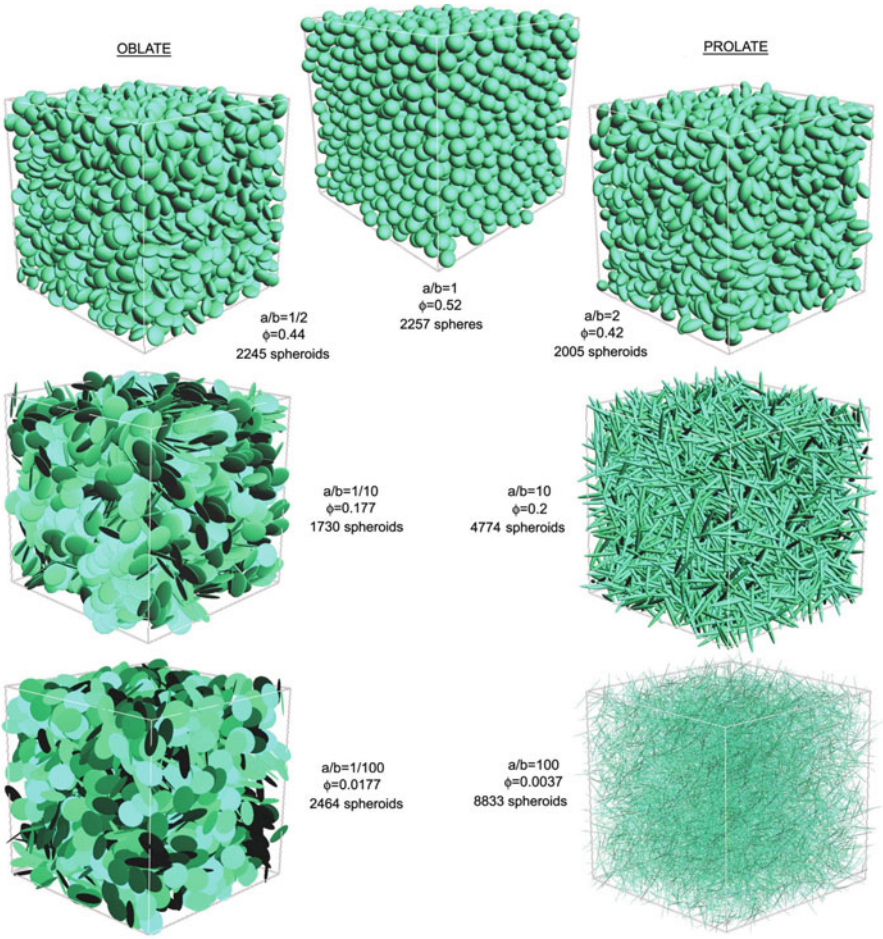

Fig. 8.4 Examples of distributions of impenetrable oblate and prolate spheroids of different aspect ratio (α/b) and volume fraction (φ) generated from computational techniques. Reprinted with permission from Ambrosetti et al. (2010)

interparticle conduction by tunnelling there must be a "well-defined" threshold. According to this and by assuming that the critical behaviour will depend on the distribution of conductance along the average local resistance of the system we can express the critical exponent as (Balberg 2012)

$$t - t_{\text{un}} = \frac{4(a-b)}{\xi} - 1$$

Although more accurate expressions of t are available (Johner et al. 2008), the above relationship is sufficient for this discussion. So far we have seen that both conductivity (under the hoping model) and the critical exponent (under the

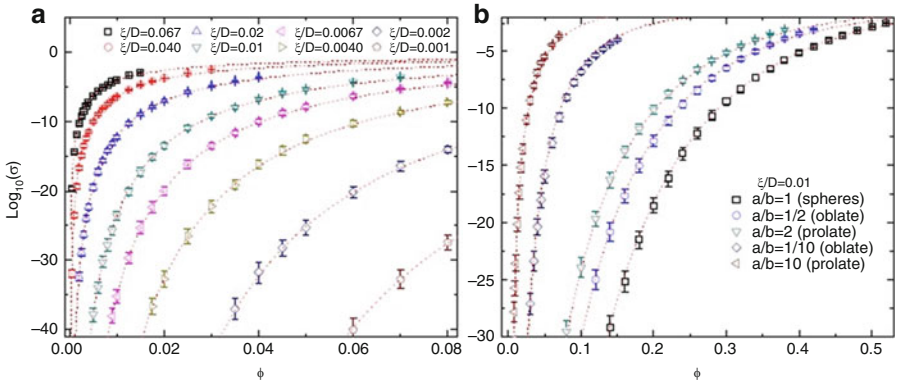

Fig. 8.5 Computational predictions indicating electrical conductivity dependence as a function of volume fraction on (**a**) tunnelling conductivity for hard prolate spheroids of aspect ratio $\alpha/b = 10$ with different characteristic tunnelling distances and (**b**) tunnelling conductivity in a system of hard spheroids of different aspect ratios. *The dotted lines* are predictions based on the critical path approximation method. Reproduced with permission from Ambrosetti et al. (2010)

tunnelling model) are dependent on the interparticle distances in the system. Therefore we can see that when conductivity varies with the concentration of particles, the effect that will dominate is the variation of the local conductance instead of the connectivity of the system. This is obviously valid only in areas where an appropriate interparticle distance distribution exists. In this description, when tunnelling is considered as the mechanism of interparticle conduction, the conductivity function $\sigma(\varphi)$ leads to two distinct results for the critical exponent (Johner et al. 2008; Balberg 2012). Based on the previous discussion we can see that the two expressions of the critical exponent behaviour are equivalent (the physics is essentially the same in both approaches) and will merge in the $(2a - 2b)/\xi \gg 1$ limit. It is also possible to estimate the percolation threshold value for prolate

$$\phi_C \approx \frac{2D}{\xi} \frac{\gamma(b/a)^2}{\ln(\sigma_o/\sigma_m)}$$

and oblate particles as a function of the matrix conductivity σ_m

$$\phi_C \approx 0.15\left(\frac{a}{b}\right)\left[\frac{2D}{\xi}\frac{1}{\ln(\sigma_o/\sigma_m)}\right]^{3/4}$$

The critical path approximation and the critical path distance δ_C are a very effective way of describing the tunnelling conductivity of polymer composites, since the geometrical connectivity problem of semi-penetrable particles in the continuum is of fundamental importance for the understanding of the filler dependencies (φ, D and α/b) on conductivity. From the above expressions for the percolation threshold (φ_C) we can see that it corresponds to the critical concentration required

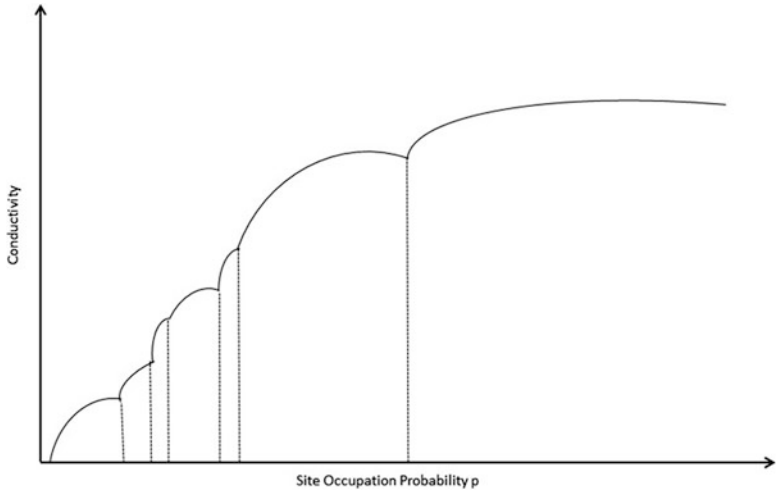

Fig. 8.6 Schematic representation of the electrical conductivity dependence on the site occupation probability when tunnelling is the main conduction mechanism. The *dotted lines* indicate the local percolation thresholds when all corresponding near neighbours are considered. The overall conductivity behaviour appears to have a staircase dependence of the occupation probability leading to a system of multiple thresholds (refer to the text for more details)

for percolation (onset of conductivity) by an ensemble of equal (or nearly equal) resistors (Balberg 2009, 2012; Balberg et al. 2004). Therefore in the tunnelling model more than just one onsets (percolations) are possible in a sequential manner, thus leading to a series of "steps" that are representative of the local conductances in the system (see Fig. 8.6). Thus in the case of a single or multiple mixed but not well-separated steps the data will be fitted with a single t in a manner similar to the standard percolation theory. In the case where multiple clearly defined steps are available multiple fits are required, leading to a larger value of t and a lower percolation threshold. In the latter case we must stress that the value of the percolation threshold does not have an intrinsic meaning.

We will close this discussion on conduction mechanisms by stressing that the tunnelling percolation model is in good agreement with experimental data and the geometrical percolation model. This is quite striking especially if we consider all the different factors that affect filler dispersion in a polymer matrix in comparison with the idealised models discussed previously. In reality fillers have non-uniform size, shape, aspect ratio and geometry distributions, and they are subject to orientation, entanglements, agglomeration and interaction with the polymer matrix. Furthermore, different mixing methods can have a huge impact on the dispersion level and structural integrity of the filler particles, especially in cases where high sheer and elongational forces are present (Gkourmpis 2014; Oxfall et al. 2015; Pötschke et al. 2004).

8.3 Filler Effects on Polymer Nanocomposites

In this section we are going to discuss the effect high aspect ratio fillers have in the polymer matrix and subsequent properties. We will discuss the effect the filler shape, size, distribution and orientation have on the polymer matrix focusing especially in the resulting morphology.

8.3.1 Aspect Ratio

High aspect ratio fillers percolate at low loadings in comparison with spherical or other low aspect ratio objects. This has been attributed to the efficiency of the network formation by large objects, due to the limited number of contacts required for the creation of a conductive cluster. This has resulted in percolation thresholds of the order of 0.1 wt% for CNT and graphene-based nanocomposites (Gkourmpis 2014; Stankovich et al. 2006; Ramasubramaniam et al. 2003; Kim and Macosko 2008; Kim et al. 2010). The theoretical percolation threshold of soft- and hard-core spheres in three dimensions is 0.29 and 0.16, respectively (Balberg 1986; Pike and Seager 1974). In the case of conventional fillers like carbon black the percolation threshold varies between 3 and 20 wt%, but these values are heavily dependent on the carbon black type, structure, surface purity and preparation method (Gkourmpis 2014). Recently, conducted theoretical studies on finite aspect ratio nanowires (Gelves et al. 2006, White et al. 2009) and randomly distributed graphite nanoplatelets (Li and Kim 2007) have highlighted the role of the aspect ratio in the percolation threshold. In both studies the filler diameter and thickness has been seen to have a direct impact on the predicted percolation threshold, and the overall aspect ratio increase leads to lower thresholds (see Fig. 8.7).

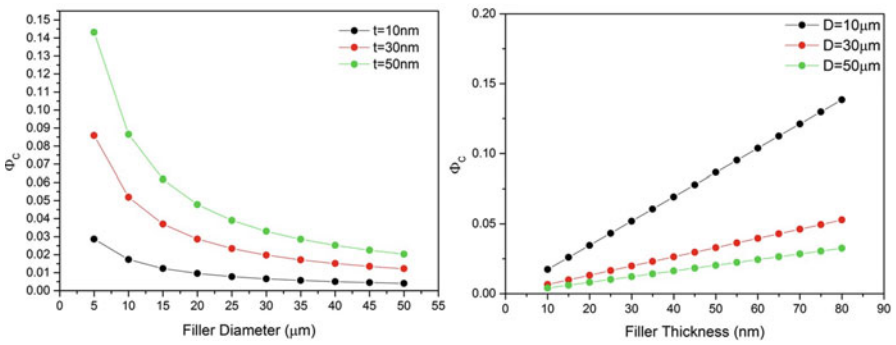

Fig. 8.7 Computational prediction on the effect of the diameter (*left*) and thickness (*right*) of randomly distributed graphene nanoplatelets of different aspect ratio (*D*/*t*) on the percolation threshold. Adopted from Li and Kim (2007)

Table 8.1 Effect of geometric shape factors and aspect ratio on the percolation threshold for graphene nanoplatelets with different matrix polymers

Polymer matrix	D (μm)	t (nm)	d/t	Percolation threshold (%vol)	Reference
High density polyethylene	6	10	600	4.46	Weng et al. (2004)
Epoxy	15	9.5	1579	1.13	Li and Kim (2007)
Poly(styrene-methyl methacrylate)	100	30	3333	0.878	Chen et al. (2001)
Polymethylmethacrylate	100	22	4545	0.529	Zheng and Wong (2003)
Polyisopropylene	50	10	5000	0.67	Chen et al. (2002)
Epoxy	46	4.5	10,222	0.5	Li et al. (2007)
Poly(ethylene vinyl-acetate)	25	6	4000	2.5	Gkourmpis (2014)
Poly(ethylene butyl-acrylate)	25	6	4000	6.9	Oxfall et al. (2015)

Here we must note that reported experimental results vary widely due to the different preparation methods that have a direct impact on the level of dispersion of the filler in the polymer matrix. All theoretical predictions are made assuming perfect or near-perfect dispersion, so a level of discrepancy between the theoretical and experimental threshold values is to be expected. These discrepancies become significant when melt mixing methods are employed. In Table 8.1 a small collection of experimental data for graphite platelets can be seen for a number of different polymers. These values are higher than the theoretical predictions seen in Fig. 8.7 indicating how important the filler geometry and preparation method is. A more comprehensive discussion on the different preparation methods and their effect on the nanocomposite properties has been presented elsewhere (Moniruzzaman and Winey 2006; Gkourmpis 2014; Kim and Macosko 2008; Kim et al. 2010).

8.3.2 Polydispersity

So far in the discussion we have assumed that all fillers introduced in the matrix are of the exact same size and shape. Such assumptions do not hold for real systems where the preparation methods of the filler and the nanocomposite have an effect on the geometry of the individual filler particle (Moniruzzaman and Winey 2006; Gkourmpis 2014; Kim and Macosko 2008; Kim et al. 2010). Carbon nanotubes especially are known to be very sensitive to their preparation methods that can have significant effects on their diameter, length and chirality. The latter is of particular importance since it has a direct influence on the electrical conductivity, resulting to metallic and semiconductive tubes (Moniruzzaman and Winey 2006). As discussed previously the aspect ratio has a strong influence on the percolation phenomena, therefore it is expected that any changes in the distribution of aspect ratio, length,

thickness (or diameter) of the filler particles will have an effect on the overall electrical conductivity of the nanocomposite.

It has been reported that the percolation threshold exhibits an inversely proportional relationship to the weight average of the length distribution in the case of rods, an effect that is getting more pronounced with increasing width of the length distribution (Kyrylyuk and van der Schoot 2008). Analytical studies predict that the incorporation of small amounts of longer rods significantly reduces the percolation threshold. This effect is also more pronounced with increasing amounts of longer rods in the system (Otten and van der Schoot 2009). The inverse relation between percolation and amount of conductive filler indicates that the electrical conductivity of the nanocomposite is governed solely by the existence of conductive particles and not the polymer matrix. Although this appears self-evident in real nanocomposites, the situation is not exactly like that. In a real system the distribution of conductivities from the high aspect ratio fillers varies in an almost continuous manner taking into consideration the morphology and the possible defects, leading to a less profound effect on the percolation than predicted theoretically. An example of this is the case of CNT-based systems, where the individual conductivity of SWCNT varies significantly, sometimes to levels of several orders of magnitude (Ebbesen et al. 1996). The contact resistance between CNTs also differs with metallic–semiconducting junctions exhibiting significantly higher values than metallic–metallic or semiconducting–semiconducting, something that has been attributed to the Schottky and tunnelling barrier between different tubes (Fuhrer et al. 2000).

The addition of low aspect ratio particles in the high aspect ratio conductive network creates a hybrid mixture of particles of different sizes. This is a common practice in both research and industrial materials as it allows for unique versatility and balancing of the overall conductivity with other desired properties of interest (e.g. viscosity, mechanical reinforcement, crystallinity). For example it has been reported that the addition of (relatively) more expensive CNTs or GNPs in standard polymer/carbon black compositions offers significant improvements in conductivity and other properties of interest (Oxfall et al. 2015; Ma et al. 2009; Sun et al. 2009; Brigandi et al. 2014; Fan et al. 2009; Wei et al. 2010; Kostagiannakopoulou et al. 2012). For epoxy and poly(ethylene butyl acrylate) copolymers it has been reported that by substituting just 10 wt% of the high aspect ratio filler (graphene nanoplatelets in this case) with carbon black a reduction of the percolation threshold from 0.75 to 0.5 wt% and 6.9 to 4.6 vol.% was achieved for the two systems, respectively (Oxfall et al. 2015; Fan et al. 2009). In a similar manner the creation of hybrid blends of graphene, nanotubes and carbon black has been seen to offer improvements in mechanical properties (Wei et al. 2010; Kostagiannakopoulou et al. 2012). The reason for the improved conductivity of hybrids has been attributed to synergistic effects between the structural arrangements of the two particle networks. Due to thermodynamic reasons it is expected that each conductive particle type will create a network structure in the matrix. This structure will have active pathways capable of enhancing conductivity and the so-called dead ends which are parts of the network that do not contribute in the overall

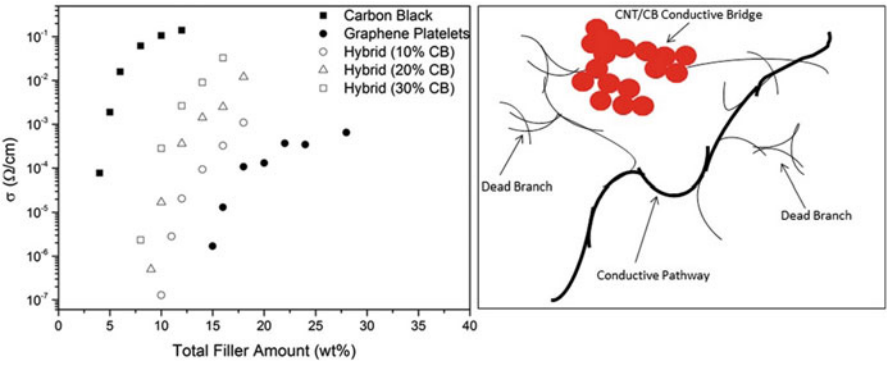

Fig. 8.8 (*Left*) Electrical conductivity as a function of filler content for EBA with carbon black, graphene platelets, and hybrid systems of mixtures between carbon black and graphene platelets. Adopted from Oxfall et al. (2015). (*Right*) schematic representation of a CB/CNT hybrid indicating the preferential localisation of the filler particles, the existence of active (conductive) and dead (non-conductive) network branches and the conductive bridges between the two filler networks existing in the matrix

conductivity. Due to size the network structure of high aspect ratio filler will be fairly extended, whereas the network of the low aspect ratio carbon black is expected to be fairly compact. Therefore, the low aspect ratio filler network can localise partially between branches of the extended high aspect ratio network creating conductive bridges (see schematic in Fig. 8.8b). By doing so the percolative behaviour of the overall composition changes, leading to a lower threshold while at the same time the overall conductivity follows a more complex expression than the traditional power law we discussed earlier. This can be seen in Fig. 8.8 where the percolative behaviour of a system of poly(ethylene butylacrylate) with carbon black and graphene nanoplatelets is presented. Both systems containing a single filler type exhibit the traditional power-law percolative behaviour, whereas the different hybrids (systems of graphene with carbon black added) deviate from it while at the same time exhibit lower percolation threshold values (Oxfall et al. 2015).

8.3.3 Orientation

All fillers are capable of orienting with external stimulus in the melt, a situation that is common in most polymer-based processes. High aspect ratio filler orientation has a far greater impact on conductivity, mainly due to the reduction of contact points between the individual particles. This contact reduction destroys the integrity of the filler network, leading to a substantial decrease in conductivity. The extent of the orientation can be described through the orientation distribution function $n(\theta, \varphi)$ and by assuming that the polar and azimuthal angles θ and ϕ are independent the

axial and planar orientation parameters for the case of rods can be expressed as (Munson-McGee 1991)

$$f_p = 2\langle \cos^2\varphi \rangle - 1$$

$$f_a = \frac{1}{3}\left(3\langle \cos^2\theta \rangle - 1\right)$$

These parameters can have values between 0 and 1 that correspond to random and axial spatial arrangement, respectively, in a matter similar to the nematic order parameter in liquid crystal polymers (both expressed in the literature as S) (Mitchell et al. 1987; Pople and Mitchell 1997; Lacey et al. 1998; Andersen and Mitchell 2013). Theoretical predictions and experimental work on nanorods in two and three dimensions have indicated that the electrical percolation takes its lowest value in the case of isotropic ($S = 0$) or slightly isotropic ($S \sim 0.1$–0.2) system. As the level of anisotropy increases the percolation threshold takes ever higher values that are correlated with the level of alignment of the filler in the system (large values of S) (Mutiso and Winey 2012; White et al. 2009; Behnam et al. 2007).

Filler orientation has a significant effect on the overall electrical conductivity especially in melt-mixing methods. This is the result of the disruption of the filler network integrity due to the shear and elongational forces during mixing. In almost all cases where the system (matrix and filler) flows the polymer chains will align along the flow direction creating extended chain conformations. This chain alignment leads to further alignment of the filler particles along the flow direction. Obviously the alignment level of the polymer is strongly dependant to the chain conformation, but in principle all polymers do exhibit a level of orientation along the flow direction. As soon as the external stimulus stops the polymer chains revert to the "natural" random coil conformations, but the filler particles due to their size cannot do the same in a very short period of time. If now we consider that in most cases when the external stimulus ends the system undergoes a certain level of cooling (e.g. injection moulding, film blowing, fibre spinning) then we can see that the crystallisation process in the matrix makes the filler movement even more difficult. Large fillers like graphene and nanotubes tend to suffer from this effect more than more traditional ones like carbon black, although this depends heavily on the shear forces and the polymer/filler composition.

8.3.4 Dispersion and Filler Localisation

Filler incorporation in a polymer matrix is achieved by a number of different methods, but all generally fall under three main categories, solution, melt and in-situ polymerisation mixing. In solution mixing, both polymer and filler dispersion is facilitated by solvents that are removed after mixing. Melt mixing is by far the most common method used commercially and in this case the filler is added to

the polymer melt and dispersion is facilitated by an external stimulus, usually in the form of a compounding or extruding machine. In the case of in-situ polymerisation mixing, the filler is added during the growth phase of the polymer. Each of the mixing methods has advantages and disadvantages, that have been discussed elsewhere (Gkourmpis 2014), but in the context of this work is sufficient to say that the level of dispersion is strongly influenced by the way the filler is incorporated in the matrix.

When filler is incorporated in a matrix, a wide range of interactions is available in the system that can have a direct link in the overall morphology, topology and properties of the nanocomposite. Polymer–filler interactions can extend over a range of distances and length-scales and can be weak or strong (Kyrylyuk and van der Schoot 2008). The interfacial energy between polymer and filler has been seen to affect the compatibility and efficiency of mixing, although this is strongly related to the chain conformation and filler structure (Alig et al. 2012). This property has been exploited in immiscible polymer blends where preferential localisation along the interface (Filippone et al. 2014; Huang et al. 2014; Gubbels et al. 1998) or in one of the phases allows for reduced percolation threshold (Gubbels et al. 1994, 1995; Gkourmpis et al. 2013). This preferential localisation enhances conductivity only in the host phase leaving part of the matrix insulating and filler free. Consequently, the overall conductivity of the nanocomposite will be determined by the conductivity of the phase that hosts the filler in a manner similar to the single polymer cases discussed previously. Obviously for the entire nanocomposite to be conductive a network is required, which means that the two polymer phases must be co-continuous. Depending on the polymers immiscible blends tend to form co-continuous phases at ranges of 30–70 %, but addition of fillers can lead to phase swelling, thus creating systems where phase continuity can be achieved at far lower amounts. An example of this is an immiscible blend of polyethylene (PE) and polystyrene (PS) that reaches co-continuity at a range of 30–45 wt% PE. The amount of PE required to create a co-continuous phase can drop to 5 wt% by addition of small amounts of carbon black (Gubbels et al. 1995). This effect is a simple manifestation of polymer thermodynamics, since the filler particle occupies a larger volume it means that the polymer phase containing it needs to take into consideration the volume increase. In terms of thermodynamics the criterion of the filler localisation and phase behaviour is the minimisation of the free energy of the system. Therefore if the free energy criterion is satisfied by the filler located in the polymer phase, then that phase will have to adjust to the volume change by swelling in a manner similar to block copolymers (Matsen 2002). If this is not possible, then the filler will localise to the larger phase that is capable of adjusting to the subsequent volume changes.

For the understanding of the percolative behaviour of conductive fillers in immiscible polymer blends, the details of the filler distribution in the different phases are important. The critical condition for achieving the all-important co-continuity of the conductive filler-rich phase has been suggested to be determined by the viscosity of the phases as (Paul and Barlow 1980)

$$\frac{\phi_A}{\phi_B} \times \frac{\eta_B}{\eta_A} = X$$

with φ and η the volume fraction and melt viscosity of the two phases (noted as A and B), respectively. For $X > 1$ phase A is continuous, $X \approx 1$ both phases are co-continuous and for $X < 1$ phase B is continuous (Jordhamo et al. 1986). Interfacial tension and wetting coefficient of the different mixture components have also been identified to influence the filler distribution and subsequent morphology of the blend. For carbon black particles in an immiscible blend it has been suggested that their distribution can be qualitatively predicted by the wetting coefficient ω. The interfacial free energy minimisation can lead to Young's equation (Sumita et al. 1991)

$$\omega_{AB} = \frac{\gamma_{CB-B} - \gamma_{CB-A}}{\gamma_{AB}}$$

with γ_{AB}, γ_{CB-A} and γ_{CB-B} the interfacial tension between polymer A and B, CB and polymer A and CB and polymer B, respectively. According to this the distribution of carbon black particles can be classified as: for $\omega_{AB} > 1$ the particles localise in phase A, for $-1 < \omega_{AB} < 1$ the particles localise along the interface and for $\omega_{AB} < -1$ the particles localise in phase B. The interfacial tension between the phases can be estimated by Wu's harmonic mean average (Wu 1982)

$$\gamma_{AB} = \gamma_A + \gamma_B - 4\left(\frac{\gamma_A^d \gamma_B^d}{\gamma_A^d + \gamma_B^d} + \frac{\gamma_A^p \gamma_B^p}{\gamma_A^p + \gamma_B^p}\right)$$

with γ_A and γ_B the interfacial tension between polymers A and B, γ_A^d and γ_B^d the dispersive components of the surface tensions γ_A and γ_B and γ_A^p and γ_B^p the equivalent polar components. According to this three spreading coefficients λ can be defined for a ternary blend (Hobbs et al. 1988)

$$\lambda_{ikj} = \gamma_{ij} - (\gamma_{ik} + \gamma_{jk})$$

Except for these thermodynamic considerations, kinetic factors, such as viscosity, chain conformation, mixing procedures (time, speed, sequence of incorporation, shear forces etc.) and possible affinity or reaction of the polymer to the filler have been seen to play a vital role in the particle localisation. Mixing in particular has been seen to have a big effect on the overall morphology of the system, as shear forces have a tendency to break large agglomerates into smaller aggregates. These smaller filler clusters can in turn erode into even smaller aggregates given enough mixing time, thus leading into a system with increased filler dispersion. Obviously such concepts are fairly simple in terms of small conductive fillers like carbon black, but the situation becomes more complicated in the case of larger nanosize and high aspect ratio fillers like graphene or nanotubes. In the latter case dispersion

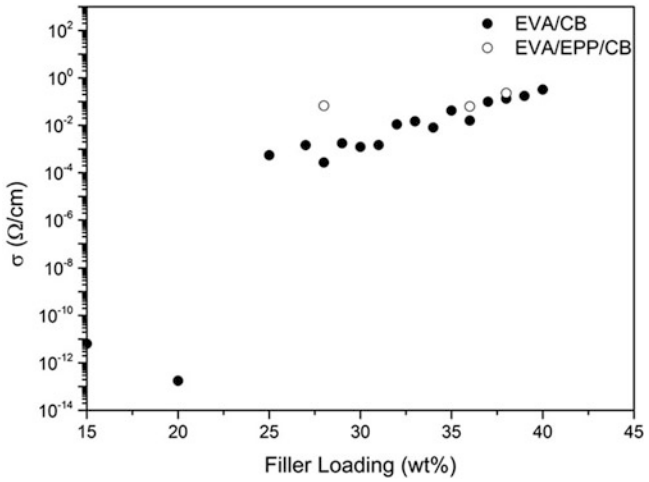

Fig. 8.9 Electrical conductivity as a function of filler loading for a system of EVA/CB and an immiscible blend of EVA/EPP/CB, indicating the effects of selective localisation. Adopted from Gkourmpis et al. (2013)

is even more difficult due to the filler size and the breakdown of the large agglomerates into smaller aggregates is truly challenging (Gkourmpis 2014).

The almost exclusive localisation of the filler in one phase of the blend has another very important effect as far as conductivity is concerned. Since the filler is the sole conductivity medium in the system (we can ignore the matrix conductivity for this discussion), its network formation will determine the amount of current flowing in the nanocomposite. As discussed previously if the system is co-continuous then the entire nanocomposite will be conductive, but its conductivity will arise *only* from the phase that contains the conductive filler. This concept is illustrated in Fig. 8.9 where the conductivity of a system of poly(ethylene vinyl-acetate)/poly(ethylene-co-propylene)/carbon black (EVA/EPP/CB) appears almost constant regardless of the filler loading (Gkourmpis et al. 2013), something that is achieved by keeping the ratio of the filler with respect to the EVA phase (where it localises) constant. In other words the percolative behaviour of the filler in the EVA phase is similar to the percolative behaviour of the same filler in the EVA phase in a single-component system.

8.3.5 Rheology and Mechanical Properties

The introduction of large conductive fillers into a polymer matrix has been seen to influence the mechanical and flow characteristics of the system. In almost all cases this addition leads to increase in storage modulus (G') and complex viscosity with increasing filling amounts (Brigandi et al. 2014). Storage modulus has been seen to

increase sharply with adding filler amounts, leading to a situation where the system crosses over from a liquid-like response to a solid-like response. This transition is usually referred to as mechanical or rheological percolation (Penu et al. 2012) and a power-law relationship can be used to determine its threshold

$$G' \propto (m - m_C)^t$$

with m the mass fraction of the filler, m_C the threshold for percolation and t the critical exponent (Du et al. 2004).

Systems containing carbon black have been seen to exhibit significant shear thinning in comparison with single polymers or binary blends. This has been utilised in the case of poly(ethylene acrylic acid) (EAA) and polypropylene (PP) blends where by adding carbon black the rheological percolation has been reported to increase with increasing EAA content. This behaviour suggested that the rheological percolation was tightly coupled with the electrical percolation by forming network structures in both PP/CB and EAA/PP/CB composites (Chen et al. 2009).

The incorporation of conductive fillers has been reported to increase the strength and stiffness of the host matrix (Gkourmpis 2014). One of the most important factors affecting the overall mechanical properties of a nanocomposite is the interfacial interaction between filler particles and polymer. This interaction is of great importance as the level of adhesion of the filler particle to the polymer will affect the efficiency of the energy transfer between them under load. In cases where the adhesion is high the stress transfer between the filler particles and the host matrix will be efficient, thus leading to an overall reinforcement of the nanocomposite. Parameters like yield, strain and tensile strength can be modelled for different adhesion levels with relatively good comparison to experimental results (Yan et al. 2006).

The reinforcement effects, as seen through the tensile strength, discussed previously are large with the incorporation of small amount of carbonaceous fillers into the polymer matrix. In the case of high aspect ratio fillers these effects are even more pronounced. The reason for this behaviour can be traced in the level of dispersion of the filler particles in the polymer matrix. In Fig. 8.10, we can see that for a system of poly(vinyl alcohol) (PVA) with graphene nanosheets introducing 0.06 vol.% of graphene into the PVA matrix the tensile strength increases by 73 % whereas by increasing the filler level from 1.8 to 3 vol.% the tensile strength increase is negligible (from 42 to 43 MPa) with the elongation at break having similar decreasing behaviour (Zhao et al. 2010). This effect has been attributed to the rearrangement and further aggregation of graphene sheets as the overall amount increases due to van der Waals interactions. When this is happening the slippage of the aggregated sheets and energy transfer to the matrix will be less efficient in comparison with the case of single sheets during a tensile measurement. In Fig. 8.10, we can see a schematic representation of this with respect to the different dispersion and aggregation levels of the filler in the matrix. Case (1) is the initial

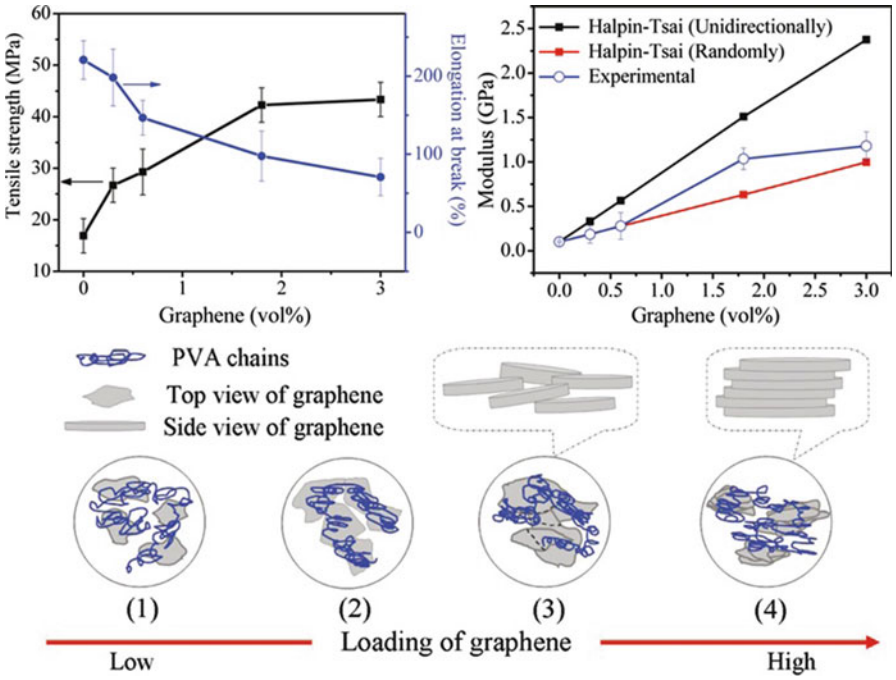

Fig. 8.10 Mechanical properties (tensile strength and elongation at break) of PVA/graphene nanocomposites as a function of graphene loading (*top left*). Comparison between experimental data of the Young's Modulus of PVA/graphene nanocomposites with theoretical predictions using the Halpin-Tsai models. Two cases of unidirectional and random distribution of the graphene in the PVA were considered for the theoretical estimations (*top right*). Schematic representation of the various levels of dispersion of graphene in the PVA. Refer to the text for a more detailed discussion of the different dispersion possibilities (*bottom*). Adopted and reprinted with permission from Zhao et al. (2010)

low loading situation where each filler particle is individually placed in the matrix, as more filler particles are introduced the spaces between the particles are filled and a network structure where the particles are in physical contact is created (case 2). Case (3) is an intermediate case where the particles are properly dispersed but a certain level of lose aggregation exists. In case (4) the individual particles are heavily aggregated creating larger structures that are detrimental to the efficiency of the reinforcement of the matrix. In a real system the spatial arrangement will move from case (1) to case (3) with increasing filler loading. A critical level of filler content called rheological (or mechanical) percolation exists on the interplay between the amount of filler and the efficiency of the mechanical reinforcement on the nanocomposite (Zhang et al. 2008). Below this content the filler particles are well dispersed and by increasing the loading a significant improvement on the mechanical performance can be realised. Above the percolation the filler particles tend to aggregate leading to inefficient structures that cannot transfer energy in an optimal manner leading to moderate mechanical improvement.

As discussed previously, a number of mathematical models for prediction of the mechanical reinforcement in polymer matrices exist. Halpin-Tsai (Halpin and Kardos 1976; Cadek et al. 2002) and Lewis-Nielsen (Lewis and Nielsen 1970) equations are based on simple approximations and provide reliable predictions of the modulus of reinforced matrices where the filler is unidirectional or randomly distributed. Therefore one can utilise these predictions to quantify the level of dispersion and the possible orientation of the filler particles in the matrix (see Fig. 8.10).

8.3.6 Crystallisation and Morphology

The introduction of conductive fillers in a polymer matrix except for the obvious effect on electrical conductivity which was discussed previously, has the possibility to affect the overall morphology of the nanocomposite. Here though we must note that the changes or their absence in the overall morphology are heavily dependent on the polymer, the type, regularity and size of the filler, the preparation methods as they affect the level of dispersion and the crystallisation conditions (Gkourmpis 2014).

For systems containing simple fillers like carbon black one expects a decrease in overall crystallinity, in comparison with the pure polymer, that is linked to the overall filler content (Gubbels et al. 1994, 1995, 1998; Gkourmpis et al. 2013). Crystallisation kinetics as seen through the melting and crystallisation temperatures are affected, something that can be attributed to the partial immobilisation of the macromolecular chains in the vicinity of the filler particles. In the case of binary blends where the filler localises in one of the two phases it is not uncommon to see morphological changes in both phases. This has been seen for a system of EVA/EPP where despite the apparent immiscibility of the two components mutual interactions between the two phases lead to the EPP phase to exhibit a split in its crystallisation peak and adopt two distinct phases. The introduction of carbon black in the system localises the particles in the EVA phase, further limiting the crystallisation of the host phase due to the reduced mobility of the polymer chains in the vicinity of the carbon black particles (Gkourmpis et al. 2013).

In the case where high aspect ratio fillers like graphene or nanotubes are introduced in the matrix the shape and geometry of the particles has been seen to have an even more direct effect on the overall crystallisation behaviour of the nanocomposite. Due to their sheer size and geometrical regularity these fillers can be very efficient nucleating agents, promoting or hindering crystallisation and leading to morphological changes (Gkourmpis 2014). CNTs have been reported to induce nanohybrid shish-kebab (NHSK) crystals for a number of polymers like PE (Laird and Li n.d.), PP (Xu et al. 2010) and poly(L-lactide) (PLLA) (Xu et al. 2011). The molecular origin of NHSK periodicity has been suggested to be closely related to the concentration gradient and the heat dissipation of the growth front of the lamellar structure. Once nucleation is initiated, the polymer concentration gradient at the crystal growth front adopts a periodic profile along the

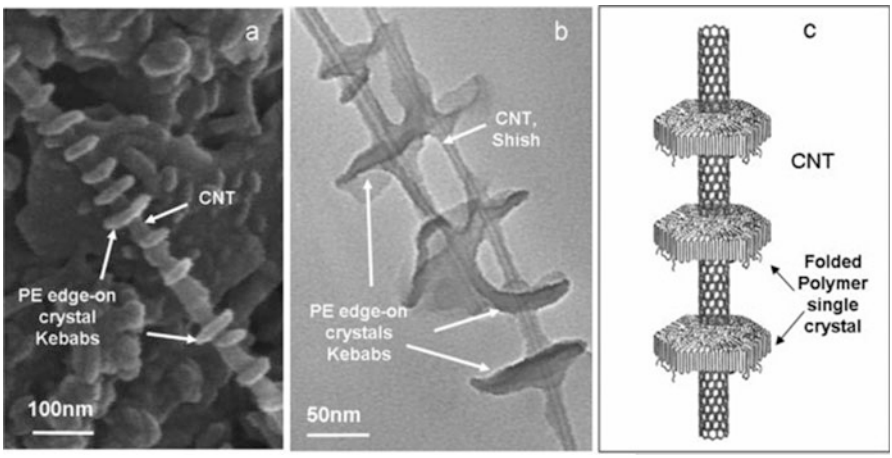

Fig. 8.11 NHSK structure of PE/MWCNT as seen by SEM (**a**), TEM (**b**) and a schematic representation indicating how lamellas grow from the CNT surface (**c**). Reprinted with permission from Li et al. (2005)

nanotube axis. This combined with the fact that most of the heat generated by the crystallisation process can be dissipated along the nanotube, leads to a further temperature gradient along the axis of the nanotube. Parameters like the crystal periodicity, the CNT diameter, the lamellar thickness and the nanotube chirality have been suggested to affect the NHSK formation and growth (Laird and Li n.d.; Li et al. 2009).

Control of the NHSK growth has been attributed to two factors, namely the epitaxial growth of the polymer on the CNT surface and the geometric confinement. Due to the small CNT dimensions the polymer chains exhibit preferential alignment along the tube axis regardless of the lattice matching between polymer and graphitic surface, leading to a soft epitaxy mechanism (Laird and Li n.d.). In the case of polyethylene the polymer behaves as being on a flat surface due to the significantly larger size of the nanotube, thus epitaxy is the main mechanism for crystal growth. As the chain begins crystallising on the surface geometric confinement, elements become important due to the comparable size of the crystal lamellar and the nanotube. Therefore the crystallisation will be preferential parallel to the nanotube axis without any regard for its chirality, leading to a situation where the orthogonal orientation of the lamellar is obtained (see Fig. 8.11) (Li et al. 2005). Computer simulations have suggested that CNT chirality is strongly influencing molecular crystallisation, something that has not so far been verified experimentally (Laird and Li n.d.).

As a final note we can say that the addition of CNTs in a semicrystalline polymer has the potential to impede, promote or have no effect on the nanocomposite crystallisation behaviour. This of course will be heavily dependent on the preparation method, the level of dispersion and the chemical configuration of both polymer and filler. It has also been suggested that the amount of CNTs in the system might

have an effect of the overall crystallisation behaviour. Low levels of CNTs might promote crystallisation while higher loadings can actually impede the whole process (Laird and Li n.d.).

In the case of graphene the two-dimensional arrangement of the filler makes lattice matching the dominant form in the crystallisation process. This can be attributed to the sequential absorption of polymer chains on the graphitic surface that leads the polymer to undergo structural rearrangements in order to adopt the lowest energy. Therefore crystallisation will take longer time something also seen experimentally in the case of polypropylene (Xu et al. 2010). The flat graphitic surface can also allow the polymer crystals to grow into multiple nucleation points and orientations. It has been suggested that the multiple spatial opportunities for crystal growth might create interference from adjacent crystals leading to an overall suppression of the crystallisation kinetics process (Xu et al. 2010). Again as in the case of nanotubes the nanocomposite preparation method, the level of filler dispersion, the amount of filler, the polymer architecture and the filler's surface characterisation are critical on the overall crystallisation process. A good example of this are two independent studies on poly(ethylene vinyl acetate) filled with graphene nanoplatelets, that indicate a totally different behaviour with respect to the crystallisation process. In the case of a melt-mixed system the existence of the filler has been seen to reduce slightly the overall crystallinity, while crystallisation takes place away from the filler that has a minimal impact on the overall morphology of the system (Stalmann 2012) in a manner similar to the one expected from traditional fillers like carbon black (Gkourmpis et al. 2013). In the case of solution-based similar systems the existence of the filler has been reported to facilitate and promote crystallisation due to the high nucleating activity of the nanoplatelets (He et al. 2011; Pang et al. 2012).

8.4 Summary

Electrically conductive polymer nanocomposites are widely used especially due to their superior properties and competitive prices. It is expected that as the level of control of the overall morphology and associated properties increases we will see an even wider commercialisation on traditional and totally novel applications. In this section we have discussed the basic principles of the percolation theory and the different types of conduction mechanisms, outlined some of the critical parameters of controlling primarily the electrical performance and we have provided some indications on the effect such conductive fillers have on the overall morphology and crystallisation of the nanocomposite. The latter becomes even more critical if we take into consideration that modern nanosized fillers offer unique potential for superior properties at low loadings (low percolation thresholds) but have a more direct impact on the morphology of the system. Furthermore we have indicated that similar systems can have totally different behaviour as the preparation methods, the chain conformation and the surface chemistry of the fillers will have a massive

impact on the resulting nanocomposite. Obviously such wide topic cannot be exhausted in a small chapter but we hope we have provided enough information to intrigue and assist the interested reader to explore this unique class of materials even further.

References

Alig I, Pötschke P, Lellinger D, Skipa T, Pegel S, Kasaliwal GR, Villmow T, Establishment T (2012) Morphology and properties of carbon nanotube networks in polymer melts. Polymer 53:4

Ambrosetti G, Grimaldi C, Balberg I, Maeder T, Danani A, Ryser P (2010) Solution of the tunneling-percolation problem in the nanocomposite regime. Phys Rev B 81:155434

E. M. Andersen, G. R. Mitchell (eds) (2013) Rheology: theory, properties and practical applications, Novapress, London 2013

Balberg I (1986) Excluded-volume explanation of Archie's law. Phys Rev B 33:3618

Balberg I (1987) Tunneling and nonuniversal conductivity in composite materials. Phys Rev Lett 59:1305

Balberg I (2009) Tunnelling and percolation in lattices and the continuum. J Phys D Appl Phys 42:064003

Balberg I, Binenbaum N (1987) Invariant properties of the percolation thresholds in the soft-core–hard-core transition. Phys Rev A 35:5174

Balberg I, Andreson C, Alexander S, Wagner N (1984) Excluded volume and its relation to the onset of percolation. Phys Rev B 30:3933

Balberg I, Yang X (eds) (2012) Semiconductive polymer composites: principles, morphologies, properties and applications. Willey-VCH Verlag, London, p 145

Balberg I, Azulay D, Toker D, Millo O (2004) Percolation and tunnelling in composite materials. Int J Mod Phys B 18:2091

Bauhofer W, kovacs JZ (2009) A review and analysis of electrical percolation in carbon nanotube polymer composites. Compos Sci Technol 69:1486

Behnam A, Guo J, Ural A (2007) Effects of nanotube alignment and measurement direction on percolation resistivity in single-walled carbon nanotube films. J Appl Phys 102:044313

Berhan L, Sastry SM (2007) Modeling percolation in high-aspect-ratio fiber systems. I. Soft-core versus hard-core models. Phys Rev E 75:041120

Berman D, Orr BG, Jaeger HM, Goldman AM (1986) Conductances of filled two-dimensional networks. Phys Rev B 33:4301

Brigandi PJ, Cogen JM, Pearson RA (2014) Electrically conductive multiphase polymer blend carbon-based composites. Polym Eng Sci 54:1

Bryning MB, Islam MF, Kikkawa JM, Yodh AG (2005) Very low conductivity threshold in bulk isotropic single-walled carbon nanotube–epoxy composites. Adv Mater 17:1186

Byrne MT, Gunko YK (2010) Recent advances in research on carbon nanotube-polymer composites. Adv Mater 22:1672

Cadek M, Coleman JN, Barron V, Hedicke K, Blau WJ (2002) Morphological and mechanical properties of carbon-nanotube-reinforced semicrystalline and amorphous polymer composites. Appl Phys Lett 81:5123

Chen GH, Wu DJ, Weng WG, Yan WL (2001) Preparation of polymer/graphite conducting nanocomposite by intercalation polymerization. J Appl Polym Sci 82:2506

Chen XM, Shen JW, Huang WY (2002) Novel electrically conductive polypropylene/graphene nanocomposites. J Mater Sci Lett 21:213

Chen G, Yang B, Guo S (2009) Ethylene–acrylic acid copolymer induced electrical conductivity improvements and dynamic rheological behavior changes of polypropylene/carbon black composites. J Polym Sci B Polym Phys 47:1762

Du F, Scogna RC, Zhou W, Brand S, Fischer JE, Winey KI (2004) Nanotube networks in polymer nanocomposites: rheology and electrical conductivity. Macromolecules 37:9048
Ebbesen TW, Lezec HJ, Hiura H, Bennett JW, Ghaemi HF, Thio T (1996) Electrical conductivity of individual carbon nanotubes. Nature 382:54
Fan Z, Zheng C, Wei T, Zhang Y, Luo G (2009) Effect of carbon black on electrical property of graphite nanoplatelets/epoxy resin composites. Polym Eng Sci 49:2041
Filippone G, Causa A, Filippone G, Causa A, de Luna MS, Sanguigno L, Acierno D (2014) Assembly of plate-like nanoparticles in immiscible polymer blends—effect of the presence of a preferred liquid–liquid interface. Soft Matter 10:3183
Fisher ME, Essam J (1961) Some cluster size and percolation problems. J Math Phys 2:609
Foygel M, Morris R, Anez D, French S, Sobolev VL (2005) Theoretical and computational studies of carbon nanotube composites and suspensions: electrical and thermal conductivity. Phys Rev B 71:104201
Fuhrer MS, Nygård J, Shih L, Forero M, Yoon Y-G, Mazzoni MSC, Choi HJ, Ihm J, Louie SG, Zettl A, McEuen PL (2000) Crossed nanotube junctions. Science 288:494
Gelves GA, Lin B, Sundararaj U, Haber JA (2006) Low electrical percolation threshold of silver and copper nanowires in polystyrene composites. Adv Funct Mater 16:2423
Gkourmpis T, Svanberg C, Kaliappan SK, Schaffer W, Obadal M, Kandioller G, Tranchida D (2013) Improved electrical and flow properties of conductive polyolefin blends: modification of poly(ethylene vinyl acetate) copolymer/carbon black with ethylene–propylene copolymer. Eur Polym J 49:1975
Gkourmpis T, Mercader GA, Haghi AK (eds) (2014) Nanoscience and computational chemistry: research progress. Apple Academic Press, Toronto, p 85
Glowacki I, Jung J, Ulanski J, Matyjaszewski K, Möller M (eds) (2012) Polymer science: a comprehensive reference, vol 2. Elsevier, London, p 847
Grimaldi C, Balberg I (2006) Tunneling and nonuniversality in continuum percolation systems. Phys Rev Lett 96:066602
Gubbels F, Jerome R, Teyssie P, Vanlathem E, Deltour R, Calderone A, Parente V, Bredas JL (1994) Selective localization of carbon black in immiscible polymer blends: a useful tool to design electrical conductive composites. Macromolecules 27:1972
Gubbels F, Blacher S, Vanlathem E, Jerome R, Deltour R, Brouers F, Teyssie P (1995) Design of electrical composites: determining the role of the morphology on the electrical properties of carbon black filled polymer blends. Macromolecules 28:1559
Gubbels F, Jerome R, Vanlathem E, Deltour R, Blacher S, Brouers F (1998) Kinetic and thermodynamic control of the selective localization of carbon black at the interface of immiscible polymer blends. Chem Mater 10:1227
Halpin JC, Kardos JL (1976) The Halpin-Tsai equations: a review. Polym Eng Sci 16:344
He F, Fan J, Lau S, Chan LH (2011) Preparation, crystallization behavior, and dynamic mechanical property of nanocomposites based on poly(vinylidene fluoride) and exfoliated graphite nanoplate. J Appl Polym Sci 119:1166
Hobbs SY, Dekkers MEJ, Watkins VH (1988) Effect of interfacial forces on polymer blend morphologies. Polymer 29:1598
Huang J, Mao C, Zhu Y, Jiang W, Yang X (2014) Control of carbon nanotubes at the interface of a co-continuous immiscible polymer blend to fabricate conductive composites with ultralow percolation thresholds. Carbon 73:267
Hunt A, Ewing R (2009) Percolation theory for flow in porous media. Springer, Berlin
Johner N, Grimaldi C, Balberg I, Ryser P (2008) Transport exponent in a three-dimensional continuum tunneling-percolation model. Phys Rev B 77:174204
Jordhamo GM, Manson JA, Sperling LH (1986) Phase continuity and inversion in polymer blends and simultaneous interpenetrating networks. Polym Sci Eng Sci 26:517
Kim H, Macosko CW (2008) Morphology and properties of polyester/exfoliated graphite nanocomposites. Macromolecules 41:3317

Kim H, Abdala AA, Macosko CW (2010) Graphene/polymer nanocomposites. Macromolecules 43:6515
Kirkpatrick S (1973) Percolation and conduction. Rev Mod Phys 45:574
Kostagiannakopoulou C, Maroutsos G, Sotiriadis G, Vavouliotis A, Kostopoulos V (2012). In: Third international conference on smart materials and nanotechnology in engineering, April 2012
Kuhner G, Voll M (1993) Manufacture of carbon black. In: Donnet J-B, Bansal RC, Wang M-J (eds) Carbon black science and technology. Taylor & Francis, London, p 1
Kyrylyuk AV, van der Schoot P (2008) Continuum percolation of carbon nanotubes in polymeric and colloidal media. Proc Nat Acad Sci USA 105:8221
Lacey D, Beattie HN, Mitchell GR, Pople JA (1998) Orientation effects in monodomain nematic liquid crystalline polysiloxane elastomers. J Mater Chem 8:53
Laird ED, Li CY (2013) Structure and morphology control in crystalline polymer–carbon nanotube nanocomposites. Macromolecules 46:2877
Lewis TB, Nielsen LE (1970) Dynamic mechanical properties of particulate-filled composites. J Appl Polym Sci 14:1449
Li J, Kim J-K (2007) Percolation threshold of conducting polymer composites containing 3D randomly distributed graphite nanoplatelets. Compos Sci Technol 67:2114
Li CY, Li L, Cai W, Kodjie SL, Tenneti KK (2005) Nanohybrid shish-kebabs: periodically functionalized carbon nanotubes. Adv Mater 17:1198
Li J, Kim JK, Sham ML, Marom G (2007) Morphology and properties of UV/ozone treated graphite nanoplatelet/epoxy nanocomposites. Compos Sci Technol 67:296
Li L, Li B, Hood MA, Li CY (2009) Carbon nanotube induced polymer crystallization: the formation of nanohybrid shish–kebabs. Polymer 50:953
Lux F (1993) Models proposed to explain the electrical conductivity of mixtures made of conductive and insulating materials. J Mater Sci 28:285
Ma PC, Liu MY, Zhang H, Wang SQ, Wang R, Wang K, Wong YK, Tang BZ, Hong SH, Paik KW, Kim JK (2009) Enhanced electrical conductivity of nanocomposites containing hybrid fillers of carbon nanotubes and carbon black. ACS Appl Mater Interfaces 1:1090
Matsen MW (2002) The standard Gaussian model for block copolymer melts. J Phys Condens Matter 14:R21
Mitchell GR, Davis FJ, Ashman A (1987) Structural studies of side-chain liquid crystal polymers and elastomers. Polymer 28:639
Moniruzzaman M, Winey KI (2006) Polymer nanocomposites containing carbon nanotubes. Macromolecules 39:5194
Munson-McGee SH (1991) Estimation of the critical concentration in an anisotropic percolation network. Phys Rev B 43:3331
Mutiso RM, Winey KI, Matyjaszewski K, Möller M (eds) (2012) Polymer science: a comprehensive reference, vol 7. Elsevier, London, p 327
Otten RHJ, van der Schoot P (2009) Continuum percolation of polydisperse nanofillers. Phys Rev Lett 103:225704
Oxfall H, Ariu G, Gkourmpis T, Rychwalski RW, Rigdhal M (2015) Effect of carbon black on electrical and rheological properties of graphite nanoplatelets/poly(ethylene-butyl acrylate) composites. eXPRESS Polym Lett 9:66
Pang H, Zhong G, Xu J, Yan D, Ji X, Li Z, Chen C (2012) Non-isothermal crystallization of ethylene-vinyl acetate copolymer containing a high weight fraction of graphene nanosheets and carbon nanotubes. Chin J Polym Sci 30:879
Paul DR, Barlow JW (1980) Polymer blends (or alloys). J Macromol Sci Rev Macromol Chem C18:109
Penu C, Hu G-H, Fernandez A, Marchal P, Choplin L (2012) Rheological and electrical percolation thresholds of carbon nanotube/polymer nanocomposites. Polym Eng Sci 52:2173
Pike GE, Seager CH (1974) Percolation and conductivity: a computer study. I. Phys Rev B 10:1421

Pople JA, Mitchell GR (1997) WAXS studies of global molecular orientation induced in nematic liquid crystals by simple shear flow. Liquid Crystals 23:467
Pötschke P, Abdel-Goad M, Alig I, Dudkin S, Lellinger D (2004) Rheological and dielectrical characterization of melt mixed polycarbonate-multiwalled carbon nanotube composites. Polymer 45:8863
Ramasubramaniam R, Chen J, Liu H (2003) Homogeneous carbon nanotube/polymer composites for electrical applications. Appl Phys Lett 83:2928
Sahimi M (1994) Applications of percolation theory. Taylor & Francis, London
Shante VKS, Kirckpatrick S (1971) An introduction to percolation theory. Adv Phys 30:325
Sherman RD, Middleman LM, Jacobs SM (1983) Electron transport processes in conductor-filled polymers. Polym Sci Eng 23:36
Shklovskii BI, Efros AL (1984) Electronic properties of doped semiconductors. Springer, Berlin
Stalmann G (2012) MSc Dissertation University of Marburg
Stankovich S, Dikin DA, Dommett GHB, Kohlhaas KM, Zimney EJ, Stach EA, Piner RD, Nguyen ST, Ruoff RS (2006) Graphene-based composite materials. Nature 442:282
Stauffer D, Aharony A (1987) Introduction to percolation theory. Taylor & Francis, London
Strumpler R, Glatz-Reichenbach J (1999) Conducting polymer composites. J Electroceram 3:329
Sumita M, Sakata K, Asai S, Miyasaka K, Nakagawa H (1991) Dispersion of fillers and the electrical conductivity of polymer blends filled with carbon black. Polym Bull 25:265
Sun Y, Bao H-D, Guo Z-X, Yu J (2009) Modeling of the electrical percolation of mixed carbon fillers in polymer-based composites. Macromolecules 42:459
Tye S, Halperin BI (1989) Random resistor network with an exponentially wide distribution of bond conductances. Phys Rev B 39:877
Wang SF, Ogale AA (1993) Simulation of percolation behavior of anisotropic short-fiber composites with a continuum model and non-cubic control geometry. Compos Sci Technol 46:389
Wei T, Song L, Zheng C, Wang K, Yan J, Shao B, Fan Z-J (2010) The synergy of a three filler combination in the conductivity of epoxy composites. Mater Lett 64:2376
Weng WG, Chen GH, Wu DJ, Yan WL (2004) HDPE/expanded graphite electrically conducting composite. Compos Interface 11:131
White SI, DiDonna BA, Mu M, Lubensky TC, Winey KI (2009) Simulations and electrical conductivity of percolated networks of finite rods with various degrees of axial alignment. Phys Rev B 79:024301
Winey KI, Vaia RA (2007) Polymer nanocomposites. MRS Bull 32:314
Winey KI, Kashiwagi T, Mu M (2007) Improving electrical conductivity and thermal properties of polymers by the addition of carbon nanotubes as fillers. MRS Bull 32:348
Wu S, Polymer (1982) interface and adhesion, M. Dekker, London
Xu JZ, Chen T, Yang CL, Li ZM, Mao YM, Zeng BQ, Hsiao BS (2010) Isothermal crystallization of poly(l-lactide) induced by graphene nanosheets and carbon nanotubes: a comparative study. Macromolecules 43:5000
Xu JZ, Chen T, Wang Y, Tang H, Li Z-M, Hsiao BS (2011) Graphene nanosheets and shear flow induced crystallization in isotactic polypropylene nanocomposites. Macromolecules 44:2808
Yan W, Lin RJT, Bhattacharyya D (2006) Particulate reinforced rotationally moulded polyethylene composites—mixing methods and mechanical properties. Compos Sci Technol 66:2080
Zhang QH, Fang F, Zhao X, Li YZ, Zhu MF, Chen DJ (2008) Use of dynamic rheological behavior to estimate the dispersion of carbon nanotubes in carbon nanotube/polymer composites. J Phys Chem B 112:12606
X. Zhao, Q. Zhang, D. Chen, P. Lu (2010). Enhanced mechanical properties of graphene-based poly(vinyl alcohol) composites. Macromolecules 43, 2357
Zheng W, Wong SC (2003) Electrical conductivity and dielectric properties of PMMA/expanded graphite composites. Compos Sci Technol 63:225